Materials Science Forum
ISSN: 1662-9752, Vol. 858, pp 1129-1132
doi:10.4028/www.scientific.net/MSF.858.1129

Submitted: 2015-07-15
Revised: 2015-11-20
Accepted: 2016-01-02
Online: 2016-05-24

Interfacial disorder of graphene grown at high temperatures on 4H-SiC(000-1)

F. Giannazzo[1,a*], G. Nicotra[1,b], I. Deretzis[1,c], A. Piazza[1,2,d], G. Fisichella[1,e], S. Agnello[2,f], C. Spinella[1,g], A. La Magna[1,h], F. Roccaforte[1,i], R. Yakimova[3,l]

[1] CNR IMM, VIII Strada 5, 95121 Catania, Italy

[2] Department of Physics and Chemistry, University of Palermo, Italy

[3] IFM, Linkoping University, Sweden

[a]filippo.giannazzo@imm.cnr.it, [b]giuseppe.nicotra@imm.cnr.it, [c]ioannis.deretzis@imm.cnr.it, [d]aurora.piazza@imm.cnr.it, [e]gabriele.fisichella@imm.cnr.it, [f]simonpietro.agnello@unipa.it, [g]corrado.spinella@imm.cnr.it, [h]antonino.lamagna@imm.cnr.it, [i] fabrizio.roccaforte@imm.cnr.it, [l]roy@ifm.liu.se

Keywords: graphene, C face, interfacial disorder, AFM, STEM, Raman

Abstract. This paper presents an investigation of the morphological and structural properties of graphene (Gr) grown on SiC(000-1) by thermal treatments at high temperatures (from 1850 to 1950 °C) in Ar at atmospheric pressure. Atomic force microscopy and micro-Raman spectroscopy showed that the grown Gr films are laterally inhomogeneous in the number of layers, and that regions with different stacking-type (coupled or decoupled Gr films) can coexist in the same sample. Scanning transmission electron microscopy and electron energy loss spectroscopy showed that a nm-thick C-Si-O amorphous layer is present at the interface between Gr and SiC. Basing on these structural results, the mechanisms of Gr growth on the C-face of SiC under these annealing conditions and the role of this disordered layer in the suppression of epitaxy between Gr and the substrate have been discussed

Introduction

The precise control over the graphitization of SiC surfaces is a key step for the production of large-scale epitaxial graphene films. While large-area growth of monolayer graphene (Gr) with a single orientation with respect to the SiC substrate has been obtained on the Si face [1,2], the growth on the C face under similar conditions typically yields an inhomogeneous film, both in the number of Gr layers, their orientation with respect to the substrate and stacking order. The differences in the morphological and electrical properties of Gr on the two polar SiC{0001} surfaces are strongly related to the growth mechanisms and the interface structure. While a single layer of C with a mixed sp^2-sp^3 hybridization (the so-called buffer layer) is observed at the interface with the (0001) face [3,4], the picture is not equally clear for Gr grown on the (000-1) face. Apart from a general acceptance of a weaker interface coupling with respect to the Si face [5], uncertainty still exists on whether Gr grows directly on the (000-1) surface [6] or if it is preceded by either ordered surface reconstructions [5] or a disordered/amorphous interface layer [7]. Recent reports have demonstrated that for high growth temperatures (>1850°C) at atmospheric pressure a nm-thick amorphous interfacial film forms between Gr and the C face of SiC [8,9].

In this paper, several morphological, structural and spectroscopic techniques, including atomic force microscopy (AFM), micro-Raman (μRaman) spectroscopy, scanning transmission electron microscopy (STEM) and electron energy loss spectroscopy (EELS), have been jointly applied to extensively investigate Gr grown at high temperatures on 4H-SiC (000-1). Atomic force microscopy (AFM) and micro-Raman (μR) spectroscopy have been used to characterize the lateral uniformity in the number of layers, the stacking-type, doping and strain. Scanning transmission electron microscopy (STEM) and electron energy loss spectroscopy (EELS) provided atomic resolution information on the interface structure and chemical composition.

Experimental

The substrates were cut out of a SI 4H-SiC (000-1) wafer with less than 0.5 degree misorientation from this direction (Cree Inc). The C-face was CMP polished and the samples were chemically cleaned before loading into the growth reactor. Gr growth was carried out by thermal annealing in inert gas (Ar) ambient at a pressure of 900 mbar within an inductively heated furnace, which allows using of high temperatures. The high temperature is beneficial for increasing the domain size of C-face grown graphene. Three different temperatures, i.e. 1850 ^{o}C, 1900 ^{o}C and 1950 ^{o}C were applied which resulted in graphene of different thicknesses, respectively. Micro-Raman measurements on as grown samples were performed with a 532 nm laser-diode source using a power <5mW. Surface morphology (topography and phase) was studied by tapping mode AFM measurements, performed with a DI3100 microscope with Nanoscope V electronics. STEM analysis were performed on cross-sectioned samples. The sample preparation procedure, including mechanical thinning followed by low-energy ion milling (3 keV), was optimized to minimize Gr delamination from SiC, C face. STEM and atomic resolution EELS measurements were performed using a sub-Angstrom aberration-corrected JEOL ARM200F microscope operated in the so-called "gentle STEM" condition, i.e. using a 60 keV primary beam energy (below the 85 keV threshold for C amorphisation [10]) in order to prevent beam-induced damage of Gr. This particular beam conditions delivered a probe size of 1.1 Å. EELS spectra were taken by scanning the electron beam in the high angle annular dark field (HAADF) STEM mode, and using ~0.75 eV spectrometer energy resolution, which was sufficient to reveal different features in the fine structure of the C-K edge, Si-L_1 and -$L_{2,3}$ edges and O-K edge.

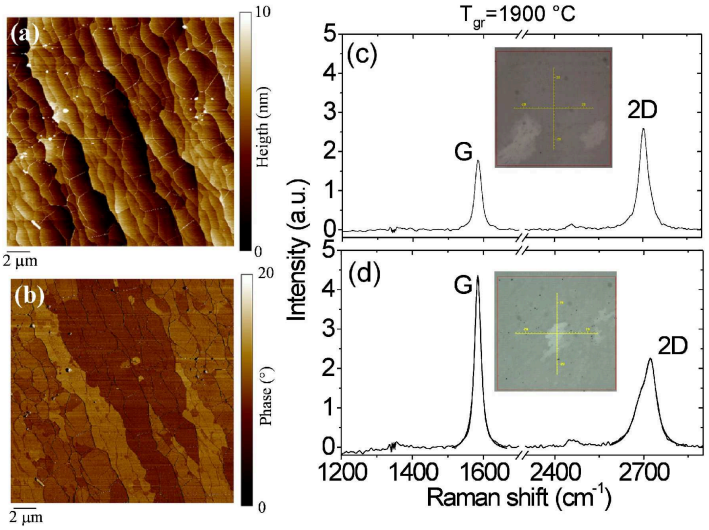

Fig. 1. AFM morphology (a) and phase (b) images of Gr grown on SiC (000-1) at 1900°C. Representative Raman spectra measured at two positions of the 1900 °C sample showing darker (c) and brighter (d) optical contrast.

Results and discussion

Representative AFM morphology and phase images for the Gr sample grown at 1900 °C are reported in Fig.1(a) and (b), respectively. The morphology shows that Gr grows on a stepped SiC substrate. The phase contrast, originating from the electrostatic interaction between tip and surface, indicates the presence of regions with different surface potential associated with changes in the number of Gr layers [11]. Fig.1(c) and (d) report two representative Raman spectra measured on the same sample at different positions showing darker and brighter optical contrast, respectively (see optical images in the inserts), corresponding to lower and higher number of layers. The absence of the defects-related D band (at ~1350 cm^{-1}) demonstrates the high crystalline quality of the few layers of Gr. While the 2D peak FWHM (~37 cm^{-1}) and the intensity ratio of the G and 2D peaks (I_G/I_{2D}≈0.7) in Fig.1(c) is consistent with the presence of a monolayer or few decoupled layers of Gr, the asymmetric shape of the 2D peak in Fig.1(d) suggests the presence of coupled Gr layers within the area of the laser spot.

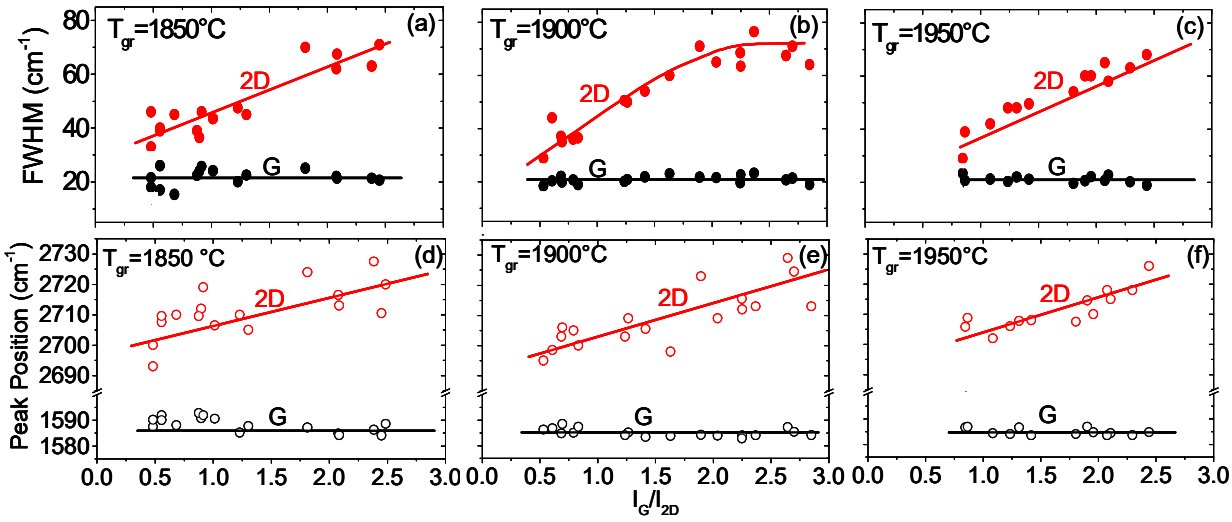

Fig.2 FWHM and peak positions of the G and 2D Raman bands and as a function of the I_G/I_{2D} ratio for Gr grown at 1850°C (a,d), 1900°C (b,e) and 1950°C (c,f).

Raman analyses were systematically performed at different positions on the Gr samples grown at 1850, 1900 and 1950°C. Fig.2(a)-(c) show the correlation between the 2D and G peaks' FWHM and the I_G/I_{2D} intensity ratio for the three different temperatures. The correlation between the G and 2D peaks' positions with I_G/I_{2D} for the three cases is depicted in Fig.2(d)-(f). For all the growth temperatures, no significant variations in the FHWM and in the position of the G peak have been observed at the different sample areas, indicating a uniform doping level in each sample [12]. On the other hand, a direct correlation between the 2D peak FWHM and the I_G/I_{2D} ratio has been observed for all the growth temperatures, which is consistent with the presence of areas with different numbers of layers in the three samples, including single layer (symmetric 2D peaks with FWHM<40 cm^{-1} and $I_G/I_{2D}\approx0.5$), decoupled few layers of graphene (symmetric 2D peaks with FWHM≈40-50 cm^{-1} and $I_G/I_{2D}\approx0.5$-1), coupled few layers of graphene (asymmetric 2D peaks with FWHM>50 cm^{-1} and $I_G/I_{2D}>1$). Clearly, the comparison of figures 2(d)-(f) indicates an increase of the average Gr film thickness with increasing the growth temperature from 1850 to 1950°C. Furthermore, a blue-shift of the 2D band with increasing the I_G/I_{2D} ratio (i.e. with the number of Gr layers) has been observed, which can be ascribed to an increasing compressive strain with increasing the Gr films thickness. This can be related to the presence of a higher fraction of domains with interlayer coupling for higher growth temperatures.

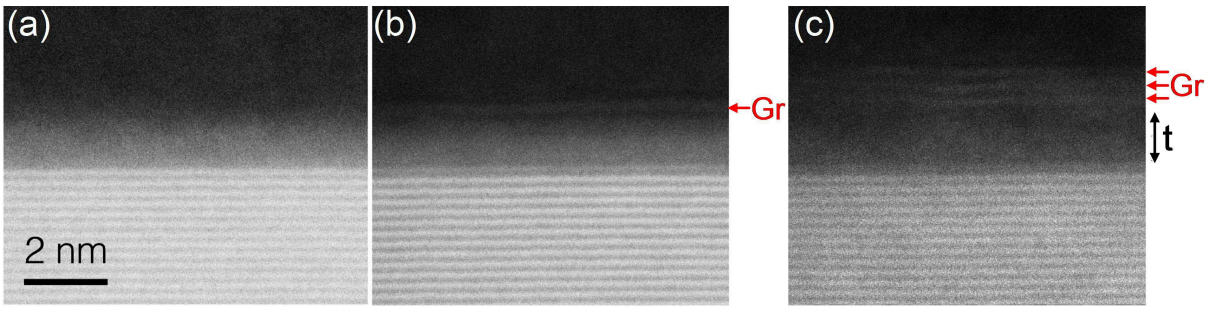

Fig.3 HAADF cross-sectional STEM images at three different areas of the Gr/SiC(000-1) interface for the sample grown at 1900 °C, showing zero (a), one (b), and three Gr layers (c) on top of an amorphous thin film with thickness t.

Three representative HAADF-STEM images acquired at different positions on the cross-section of the sample are reported in Fig.3, showing zero (a), one (b), and three (c) Gr layers on top of a thin amorphous film at the interface with SiC. For the sample grown at 1900 °C, this amorphous region has fixed thickness (~1.1 nm) both on the bare and Gr covered regions, almost independently on the

number of Gr layers. Interestingly, the thickness of this interfacial layer is found to be lower in the samples grown at lower temperature (1850 °C).
Fig.4 shows a cross-sectional HAADF-STEM (a) and atomic resolution EELS analyses performed in the spectral regions of Si-L (b), C-K (c) and O-K (d) edges at different positions on the cross section of the sample grown at 1900°C. Clearly, the Si-L spectral contributions (Fig.4(b)) are prominent in the two topmost SiC layers, whereas their intensity gradually decreases within the amorphous film moving from the interface with SiC to the first Gr layer, where it drops to zero. The C-K edge spectrum (Fig.4(c)) clearly shows the presence of C in the amorphous film, and the occurrence of sp^2 hybridization (featured by a sharp π* component) in the 1st and 2nd Gr layers.
Finally, the O-K spectra in Fig.4(d) indicate oxygen presence within this amorphous layer, whose incorporation (during or after Gr growth) is still matter of discussion.
This structural analyses suggests growth process that starts with the formation of the amorphous layer at the SiC surface and moves toward the bulk of SiC as Si atoms sublimates. Gr layers form by the conversion of C on top of this amorphous layer to sp^2 film. Within this scheme, new Gr layers should form below the existing ones as soon as the available C concentration allows it.

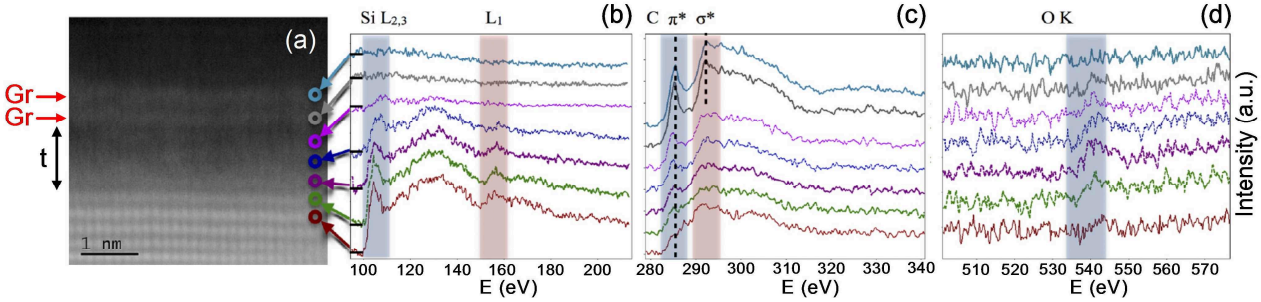

Fig. 4. HAADF cross-sectional STEM image (a) and local EELS spectra acquired in the spectral regions of Si-L edge (b), C-K edge (c) and O-K edge (d).

Summary

This study showed that laterally inhomogeneous Gr films are obtained by high temperature annealing of SiC(000-1), with a number of Gr layers ranging from a monolayer to multilayers, and the coexistence of regions with decoupled Gr layers and regions where Gr layers are coupled. A nm-thick C-Si-O amorphous layer is observed at the interface between Gr and SiC, whose thickness is independent on the number of the overlying Gr layers. From a compositional point of view, this layer is inhomogeneous in the depth direction, as its Si concentration gradually decreases while approaching the surface. Clearly the presence of this layer interfacial layer between SiC(000-1) and Gr plays a key role in suppressing the epitaxy in this heterostructrure.

References

[1] K. V. Emtsev, et al, Nat. Mater. 8 (2009) 203.
[2] C. Virojanadara, et al, Phys. Rev. B 78 (2008) 245403.
[3] K. V. Emtsev, et al, Phys. Rev. B 77 (2008) 155303.
[4] G. Nicotra, et al. , ACSNano 7 (2013) 3045.
[5] F. Hiebel, et al., Phys. Rev. B 78 (2008) 153412.
[6] J. Borysiuk, et al., J. Appl. Phys. 108 (2010) 013518.
[7] R. Colby, et al., Appl. Phys. Lett. 99 (2011) 101904.
[8] C. Bouhafs, et al., J. Appl. Phys. 117 (2015) 085701.
[9] G. Nicotra, et al., Phys. Rev. B 91 (2015) 155411.
[10] O. L. Krivanek, et al., Nature 464 (2010) 571.
[11] C. Vecchio, et al., Nanoscale Research Letters 6 (2011) 269.
[12] A. Das, et al. Nature Nanotechnology, 3, (2008) 210-215.